

# Vanilloid Receptor–Related Osmotically Activated Channel (VR-OAC), a Candidate Vertebrate Osmoreceptor

Wolfgang Liedtke,\* Yong Choe,†  
Marc A. Martí-Renom,‡ Andrea M. Bell,†§  
Charlotte S. Denis,†§ Andrej Šali,‡  
A. J. Hudspeth,†§ Jeffrey M. Friedman,\*§  
and Stefan Heller†||

\*Laboratory of Molecular Genetics

†Laboratory of Sensory Neuroscience

‡Laboratory of Molecular Biophysics

§Howard Hughes Medical Institute

The Rockefeller University

1230 York Avenue

New York, New York 10021

## Summary

The detection of osmotic stimuli is essential for all organisms, yet few osmoreceptive proteins are known, none of them in vertebrates. By employing a candidate-gene approach based on genes encoding members of the TRP superfamily of ion channels, we cloned cDNAs encoding the vanilloid receptor–related osmotically activated channel (VR-OAC) from the rat, mouse, human, and chicken. This novel cation-selective channel is gated by exposure to hypotonicity within the physiological range. In the central nervous system, the channel is expressed in neurons of the circumventricular organs, neurosensory cells responsive to systemic osmotic pressure. The channel also occurs in other neurosensory cells, including inner-ear hair cells, sensory neurons, and Merkel cells.

## Introduction

Most organisms are sensitive to osmotic and mechanical stimulation (French, 1992). This responsiveness is thought to be mediated by ion channels that measure the tension in membranes (Kernan and Zuker, 1995; Sackin, 1995) or in other elastic elements (Hudspeth and Gillespie, 1994). Stretch-activated channels have been isolated from bacteria and their molecular structure has been reported (Sukharev et al., 1994). A stretch-sensitive channel has also been identified in yeast (Kanzaki et al., 1999); like the bacterial channels, this may be involved in sensing osmotic stimuli. Finally, a group of genes have been shown by genetic approaches in *Caenorhabditis elegans* and *Drosophila melanogaster* to encode putative ion channels involved in mechanosensation (*mec-4*, *mec-10*, *Osm-9*, and *NompC*; Gu et al., 1996; Lai et al., 1996; Colbert et al., 1997; Walker et al., 2000). Mutations in these genes cause variously loss of osmotic avoidance, touch insensitivity, lack of responsiveness to sound, and dyscoordination through impaired proprioception.

Because no genes encoding osmotically or mechanically activated ion channels have been identified in vertebrates, we undertook a search for mammalian and avian homologs of OSM-9. We describe here a vertebrate osmotically gated ion channel that is related to OSM-9 and to the vanilloid receptor 1 (VR1; Caterina et al., 1997). The functional properties of this channel upon heterologous expression in eukaryotic cells, as well as its gene expression pattern, suggest that it is an osmoreceptor involved in the regulation of systemic osmotic pressure.

## Results

### Molecular Cloning of VR-OAC

In an attempt to identify osmoreceptive and mechano-sensitive ion channels in vertebrates, we sought vertebrate homologs of the *C. elegans* gene *Osm-9*, whose product confers sensitivity to osmotic pressure, touch, and specific odorants (Colbert et al., 1997). We also used sequence information about two vertebrate proteins with significant similarity to OSM-9, the vanilloid receptor VR1, which responds to vanilloid ligands, and the vanilloid receptor-like receptor VRL-1, which is activated by noxious temperatures (Caterina et al., 1997; Caterina and Julius, 1999; Caterina et al., 1999).

Expressed-sequence tags encoding vertebrate proteins homologous to OSM-9 and VR1 were identified in GenBank and employed as probes for high-stringency screening of a rat kidney cDNA library. This approach resulted in the isolation of a cDNA of 3211 base pairs that includes an open reading frame of 2613 nucleotides. In a complementary strategy, a mixture of nucleotide probes corresponding to the transmembrane regions of OSM-9, VR1, and VRL-1 was used for low-stringency screening of a mouse hypothalamic cDNA library and of an arrayed chicken inner-ear cDNA library (Heller et al., 1998). This led to the isolation of murine and chicken cDNAs homologous to the rat cDNA. Finally, the sequence of the human ortholog was retrieved from the high-throughput genomic-sequence database (GenBank accession number AC007834) and completed by PCR-based cloning from HEK293 cell cDNA.

The novel protein identified in the four species has the primary structural characteristics of an ion channel and is named VR-OAC, for vanilloid receptor–related osmotically activated ion channel. The predicted amino acid sequences of VR-OAC from the four species are depicted in Figure 1. Hydrophobicity analysis of VR-OAC indicates a structure similar to those of OSM-9, VR1, and VRL-1, with six predicted membrane-spanning domains and a putative pore loop (Figure 2A). VR-OAC's amino-terminal domain bears three ankyrin repeats and, like its carboxyl terminus, is predicted to occur intracellularly. Analysis of phylogenetic relationships indicates that VR-OAC represents a member of the OSM-9 family in the TRP superfamily of ion channels (Figure 2B; Harteneck et al., 2000).

|| To whom correspondence should be addressed at the following present address: Eaton-Peabody Laboratory, Massachusetts Eye and Ear Infirmary and Harvard Medical School, 243 Charles Street, Boston, Massachusetts 02114 (e-mail: hellers@epl.meei.harvard.edu).

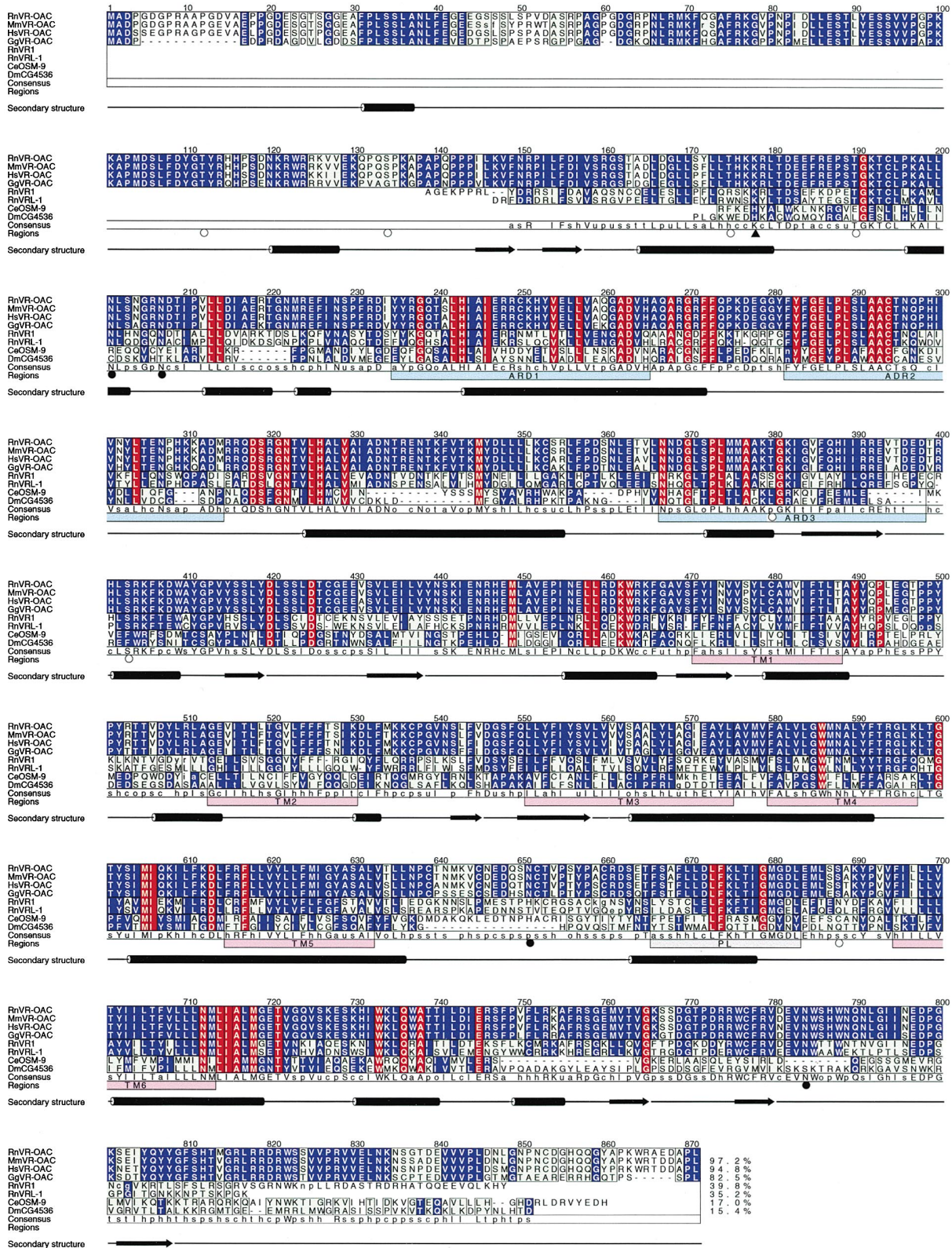


Figure 1. Analysis of VR-OAC Amino Acid Sequences

Comparison of the amino acid sequences for VR-OAC from the rat (Rn; 871 amino acids), mouse (Mm; 873 amino acids), human (Hs; 871 amino acids), and chicken (Gg; 852 amino acids) with related proteins, including RnVR1, RnVRL-1, *Caenorhabditis elegans* (Ce) OSM-9 (GenBank accession number AF031408), and its putative *Drosophila melanogaster* (Dm) ortholog CG4536 (GenBank accession number AAF46203). Amino acid residues are numbered from the first methionine of RnVR-OAC. The amino and carboxyl termini of RnVR1, RnVRL-1, OSM-9, and CG4536 that do not align with the VR-OACs are omitted. Lowercase letters denote the first and last residues of insertions with

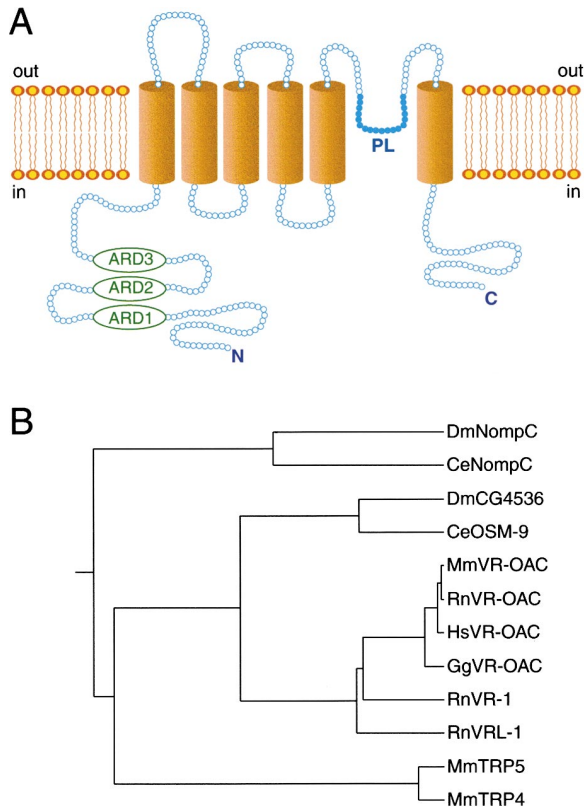


Figure 2. Schematic Structure and Phylogenetic Relations of VR-OAC

(A) Schematic structure of VR-OAC predicted by hydropathy analysis. Three ankyrin-repeat domains (ARD) occur near the amino terminus. The channel's core comprises six  $\alpha$ -helical transmembrane domains and a pore loop (PL).

(B) The phylogenetic relations among VR-OAC-related proteins, including NOMPc and mammalian TRP proteins. The species abbreviations are provided in the caption of Figure 1.

#### Chromosomal Location of *Vroac* and *Vr1* Genes

We identified genomic sequence-tagged sites flanking the human *VROAC* locus and mapped the gene to chromosome 12q24 between the markers D12S1339 and D12S2291. Because the human *VR1* gene is located on chromosome 17 (Touchman et al., 2000), *VR-OAC* and *VR1* stem from separate but related genes, rather than from splice variants of the same gene.

To establish the map positions of these genes in the mouse, we typed a radiation-hybrid panel and a BSS interspecific cross from the Jackson Laboratory with probes corresponding, respectively, to *Vroac* and *Vr1*. *Vroac* mapped to the distal arm of chromosome 5 between the anchored markers D5Mit25 and D5Mit188;

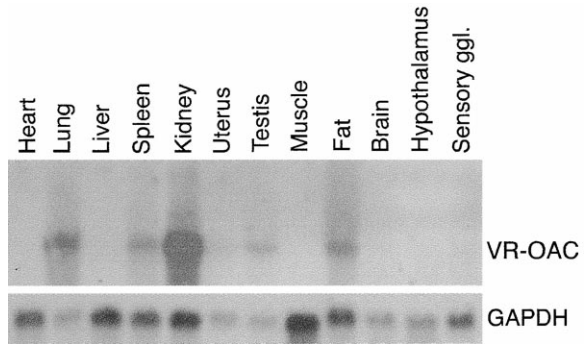


Figure 3. VR-OAC mRNA Expression in Rat Organs

A multiple-organ Northern blot demonstrates expression of a 3.2 kb VR-OAC mRNA in lung, spleen, kidney, testis, fat, and faintly in trigeminal ganglia. The upper panel shows an autoradiograph of the membrane hybridized with a VR-OAC-specific probe. As an indicator of the relative mRNA loading, the lower panel shows the signal after hybridization to detect the mRNA of glyceraldehyde 3-phosphate dehydrogenase.

*Vr1* was localized on chromosome 11 between D11Mit7 and D11Mit36. The map positions for both genes represent chromosomal locations with conserved synteny between the murine and human genomes.

#### Expression of VR-OAC

To determine the expression pattern of VR-OAC, we first performed Northern blot analysis (Figure 3). A single mRNA species of 3.2 kb was abundant in kidney, lung, spleen, testis, and fat. A lower level of expression was observed in sensory ganglia. When polyA<sup>+</sup> RNA from 150 mouse cochleae was subjected to Northern blot analysis, a faint 3.2 kb band of VR-OAC mRNA was detected (not shown).

A more detailed analysis of VR-OAC expression was performed by *in situ* hybridization. Although relatively faint signals are characteristically associated with low-abundance messages such as those for ion channels, we detected VR-OAC mRNA in several sites. In the central nervous system, VR-OAC was expressed in neurons of two circumventricular organs, the vascular organ of the *lamina terminalis* (VOLT) and the subfornical organ (SFO; Figures 4A, 4B, and 4D). The median preoptic area (MnPO) of the *lamina terminalis* also contained labeled neurons (Figures 4A and 4D). VR-OAC mRNA occurred in ependymal cells lining the choroid plexus of the lateral ventricles (Figures 4C and 4D); the ependymal cells of the third ventricle, on the contrary, did not express VR-OAC (Figure 4A). Scattered neurons in other regions of the brain, including the cerebral cortex, thalamus, hippocampus, and cerebellum, expressed VR-OAC mRNA

respect to the RnVR-OAC sequence. Red columns highlight positions with identical residues over all sequences. Blue columns indicate positions with identical residues within sequence groups (the VR-OACs, RnVR1 and RnVRL-1, and OSM-9 and CG4536). Cyan columns denote conserved positions. The last alignment row shows the consensus sequence. The lowercase characters indicate conservation of chemical classes: o = alcohol, l = aliphatic, a = aromatic, c = charged, h = hydrophobic, p = polar, s = small, u = tiny, and t = turnlike. The percentage of sequence identity of each sequence to the RnVR-OAC sequence is shown at the end of the alignment. Ankyrin-repeat domains (ARD, pale blue boxes), transmembrane regions predicted by PHDhtm (TM, magenta boxes), putative pore-loop regions (PL, gray box), and the secondary structures predicted for RnVR-OAC by PHDsec are indicated. The triangle indicates a putative cAMP-dependent phosphorylation site, open circles denote predicted PKC phosphorylation sites, and filled circles indicate possible asparagine glycosylation sites.

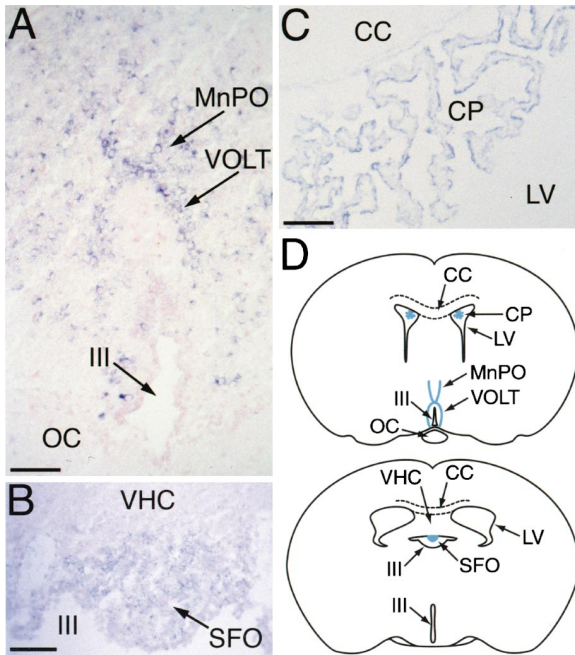


**Figure 4.** In Situ Hybridization Analysis of VR-OAC Expression in the Central Nervous System

(A) In a coronal section of the *lamina terminalis* of the mouse brain, VR-OAC-expressing neurons occur in the arched vascular organ of the *lamina terminalis* (VOLT). Positive neurons are also located in the median preoptic area (MnPO); a few labeled neurons are scattered through the adjacent brain. The optic chiasm (OC) lies below the third ventricle (III), whose ependymal cells are unlabeled.

(B) In another coronal section of the murine *lamina terminalis*, VR-OAC mRNA is abundantly expressed in neurons of the subformal organ (SFO). VHC, ventral hippocampal commissure.

(C) The ependymal cells of the choroid plexus (CP) of the rat's lateral ventricle (LV) express VR-OAC mRNA. CC, *corpus callosum*.

(D) Two orientation drawings situate the structures in panels (A)–(C) in coronal sections of the rodent brain. The abbreviations are as noted for those illustrations.

The sections in panels (A)–(C) were lightly counterstained with nuclear fast red. The scale bars correspond to 50  $\mu$ m.

weakly (not shown). For these and all the other in situ results presented, sense controls were uniformly negative (not shown).

In the mouse's inner ear, VR-OAC was expressed in both inner and outer hair cells of the organ of Corti (Figure 5A) as well as in hair cells in the cristae of the semicircular canals and in the utricular macula (not shown). VR-OAC mRNA also occurred in large cell bodies of the auditory ganglion and in marginal cells of the *stria vascularis* (Figure 5B). Similar results were obtained for avian VR-OAC in the chicken's inner ear.

VR-OAC mRNA was abundantly expressed in the trigeminal ganglion in a subpopulation of sensory neurons with large somata (Figure 5C). We also detected expression in Merkel cells within the sinuses of vibrissae on the snout (Figure 5D).

In the kidney, VR-OAC mRNA was found in tubular epithelial cells; a significantly weaker signal was also apparent in glomeruli (Figure 5E).

#### Osmotic Gating of VR-OAC

To confirm that VR-OAC functions as an ion channel and to determine the stimulus that gates it, we expressed the

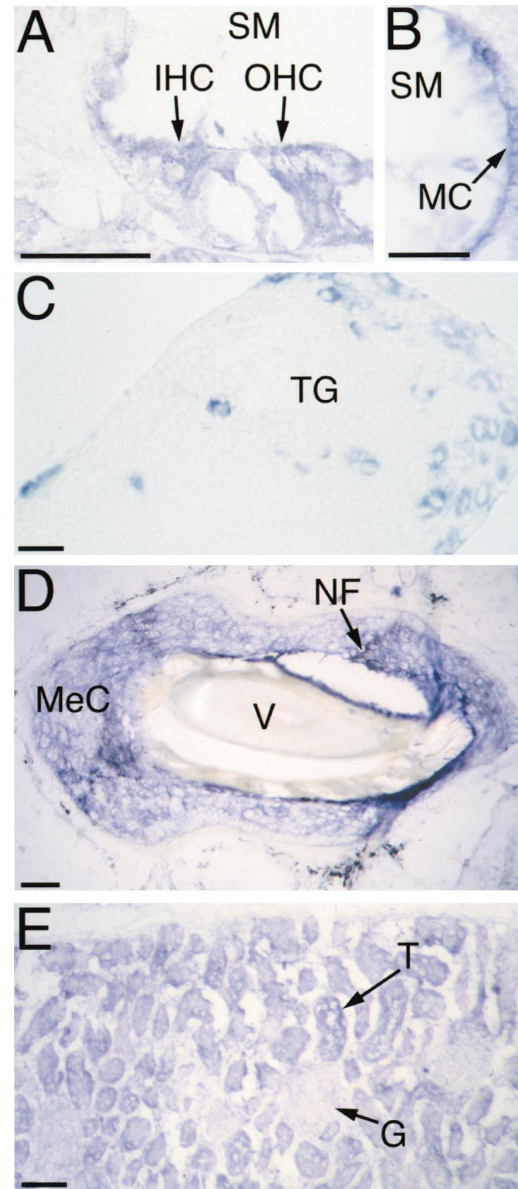


**Figure 5.** In Situ Hybridization Analysis of Rodent VR-OAC Expression

(A) In the murine cochlea, VR-OAC mRNA occurs in both inner hair cells (IHC) and outer hair cells (OHC). SM, *scala media*.

(B) Marginal cells (MC) of the cochlear *stria vascularis* in the mouse display VR-OAC mRNA.

(C) In the murine trigeminal ganglion (TG), VR-OAC mRNA occurs in a population of large neurons. Specific staining is not detectable in small and very large sensory ganglion cells.

(D) Surrounding the obliquely sectioned shaft of a vibrissa (V) from an albino rat's snout, Merkel cells (MeC) strongly express VR-OAC (blue reaction product). Nerve fibers (NF) innervating the Merkel cells are black following antineurofilament immunolabeling.

(E) In the cortex of the murine kidney, VR-OAC is strongly expressed by epithelial cells of tubules (T). The expression in glomeruli (G) is much weaker.

The scale bars correspond to 50  $\mu$ m.

rat and chicken proteins in stably transfected Chinese hamster ovary (CHO) cells. Untransfected CHO cells and a line stably transfected with a VR1-expressing plasmid served as controls. We loaded VR-OAC-expressing cells

with the  $\text{Ca}^{2+}$ -indicator fluo-4 AM and used conventional and confocal microscopy to monitor changes in fluorescence, which reflected alterations in the intracellular  $\text{Ca}^{2+}$  concentration.

Upon osmotic stimulation of transfected cells, intracellular fluorescence increased significantly within seconds under hypotonic but not hypertonic conditions (Figure 6A, upper panels). Cells expressing the rat and the chicken orthologs were indistinguishable in their responsiveness. A control cell line expressing rat VR1 did not respond to changes in osmotic strength but did display strong  $\text{Ca}^{2+}$  influx after exposure to the vanilloid hyperagonist resiniferatoxin (Figure 6A, lower panels). Individual transfected cells displayed two response patterns during exposure to hypotonic conditions. Some cells had elevated intracellular  $\text{Ca}^{2+}$  levels throughout the exposure (Figure 6B, upper trace). Other cells showed oscillating intracellular  $\text{Ca}^{2+}$  concentrations (Figure 6B, lower trace) with as many as eight cycles of increased fluorescence during a 2 min stimulus period.

If VR-OAC is naturally gated by changes in the transmembrane osmotic pressure, one would expect the channel to respond to minute fluctuations. We confirmed this by observing responses as the osmotic strength of the extracellular medium was decreased in small increments (Figure 6C). VR-OAC-mediated  $\text{Ca}^{2+}$  influx was detectable even upon exposure to an osmotic strength of  $292 \text{ mmol}\cdot\text{kg}^{-1}$ , a deviation of only 1% from the control value (not shown).

We performed additional experiments to test the specificity of VR-OAC's response to osmotic stimuli. Because chicken and rat VR-OAC-transfected cells did not respond to isotonic reduction of the  $\text{Na}^+$  concentration to as low as 50 mM, the channel is unlikely to sense hyponatremia. The cells responded neither to the vanilloid hyperagonist resiniferatoxin nor to anandamide, an endogenous cannabinoid and agonist of human and rodent VR1 (Zygmunt et al., 1999). Furthermore, no response was observed upon exposure of VR-OAC-transfected cells in isotonic medium to temperatures ranging from room temperature to  $55^\circ\text{C}$ .

The sensitivity of VR-OAC to osmotic stimulation was noticeably increased at physiological temperatures (Figure 6D). Interestingly, the temperatures of greatest responsiveness differed between the rat and chicken VR-OACs. The maximal sensitivity of the rat VR-OAC occurred at the mammalian core body temperature of  $37^\circ\text{C}$ . For the chicken VR-OAC, maximal responsiveness corresponded to the avian core body temperature of  $40^\circ\text{C}$  (Eppley, 1996). At  $40^\circ\text{C}$ , the difference in increase of  $\text{Ca}^{2+}$  influx between rat and chicken VR-OACs was statistically significant ( $p = 0.03$ , Student's *t* test). VR-OAC is therefore capable of detecting small osmotic-pressure changes under physiological conditions.

#### Origin of VR-OAC-Induced $\text{Ca}^{2+}$ Signals

The large and often oscillatory  $\text{Ca}^{2+}$  signals observed after stimulation of VR-OAC-transfected cells suggest responses amplified by the release of  $\text{Ca}^{2+}$  from internal stores, which is known to occur in CHO cells (Penner et al., 1989). To confirm this possibility, we depleted internal stores in control experiments by opening  $\text{IP}_3$ -gated channels with thapsigargin; we additionally prevented  $\text{Ca}^{2+}$  replenishment by blocking potentiation

channels with SKF 96365 (Merritt et al., 1990). Under these conditions, hypotonic stimuli failed to further increase the slightly elevated background level of  $\text{Ca}^{2+}$ -induced fluorescence (Figure 6E). These results suggest that VR-OACs do not admit most of the  $\text{Ca}^{2+}$  that appears in the cytoplasm upon osmotic stimulation, but rather trigger  $\text{Ca}^{2+}$  release from intracellular stores.

We next sought to determine whether  $\text{Ca}^{2+}$  release from internal stores is triggered by  $\text{Ca}^{2+}$  entering the cells through open VR-OACs. When loaded with fluo-4 AM in isotonic saline solution without  $\text{Ca}^{2+}$ , VR-OAC-transfected cells displayed only low baseline fluorescence (Figure 6F). No change in fluorescence was apparent upon substitution of hypotonic solution lacking  $\text{Ca}^{2+}$ ; subsequent addition of 2 mM  $\text{Ca}^{2+}$  led within a few seconds to a strong increase of intracellular fluorescence.

Two other experiments buttressed the conclusion that  $\text{Ca}^{2+}$  entering through VR-OACs triggers internal release. First, the fluo-4 fluorescence did not increase upon depolarization of VR-OAC-transfected cells by addition of 20 mM  $\text{K}^+$  to  $\text{Ca}^{2+}$ -containing isotonic medium. It follows that neither depolarization per se nor any subsequent transmembrane flux of  $\text{Na}^+$  or  $\text{K}^+$  suffices to trigger release. Second, when transfected cells were maintained in a solution in which the  $\text{Na}^+$  and  $\text{K}^+$  had been replaced by 120 mM of the impermeant cation *N*-methyl-D-glucamine, but the  $\text{Ca}^{2+}$  concentration remained 2 mM, an increase in fluorescence occurred upon exposure to hypotonic solution of otherwise identical composition (not shown). These control experiments establish that  $\text{Ca}^{2+}$  entry through VR-OACs is both necessary and sufficient to evoke internal  $\text{Ca}^{2+}$  release, but do not exclude the possibility that additional molecular signals intervene in the process.

#### Electrophysiological Characterization of VR-OAC

We evaluated the properties of VR-OAC by tight-seal recordings from transfected cells. Consistent with the fluorescence imaging experiments, hypotonic stress of cells during whole-cell recording induced channel opening within a few seconds to 2 min, whereas isotonic stasis or hypertonic conditions did not (Figure 7A). Reversal-potential measurements indicated that the channel's permeability to  $\text{K}^+$  slightly exceeds that to  $\text{Na}^+$  and that the permeability to  $\text{Cl}^-$  is substantially lower.

VR-OACs displayed the dual rectification (Figure 7B) found in some other members of the TRP superfamily (Caterina et al., 1999). Because we used EDTA to lower divalent-cation concentrations into the nanomolar range and maintained identical ionic compositions for internal and external solutions, rectification may be an intrinsic property of VR-OAC, rather than a consequence of divalent-cation blockage. Extracellular  $\text{Ca}^{2+}$  evoked a pronounced outward rectification by greatly reducing the inward current (Figures 7A and 7B). This rapid and reversible response suggests that  $\text{Ca}^{2+}$  produces a flicker block of the channel's pore.  $\text{Ca}^{2+}$  exposure also increased the outward current relative to that seen in the standard hypotonic solution. This response, which was rapid, reversible, and reproducible across many cells, betokens an additional  $\text{Ca}^{2+}$ -dependent modulation of the channel.

Gadolinium ion ( $\text{Gd}^{3+}$ ) blocks the activity of many

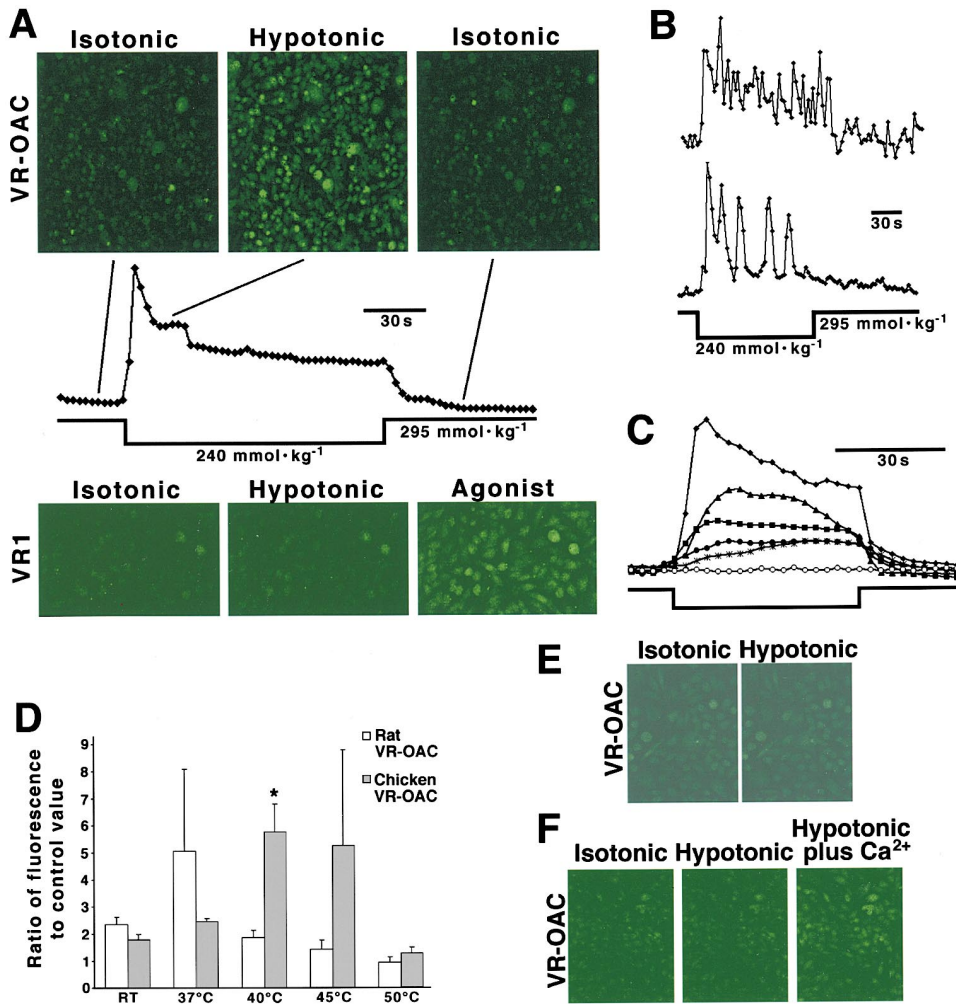


Figure 6. Gating of VR-OAC Investigated by Ca<sup>2+</sup> Imaging

(A) CHO cells, permanently transfected with an expression vector for chicken VR-OAC and loaded with the Ca<sup>2+</sup>-indicator fluo-4, are observed by confocal microscopy. Replacement of the isotonic extracellular solution (295 mmol·kg<sup>-1</sup>) with hypotonic medium (245 mmol·kg<sup>-1</sup>) results in a dramatic increase in fluorescence, reflecting a rise in the intracellular Ca<sup>2+</sup> concentration (upper panels). Replacement of isotonic solution restores the Ca<sup>2+</sup> concentration to its background level. In a quantitative analysis of frames from the series, each point represents the fluo-4 fluorescence from a microscopic field containing approximately 2000 cells (plot). The peak fluorescence is 3.8× as great as the control value. Control cells expressing rat VR1 do not exhibit alterations of intracellular Ca<sup>2+</sup> concentration when the osmotic strength is changed (lower panels). Exposure to 200 nM of the vanilloid agonist resiniferatoxin increases the intracellular Ca<sup>2+</sup> concentration.

(B) Individual cells respond to hypotonic solution either by an elevated Ca<sup>2+</sup> concentration throughout the stimulus period (upper trace) or by an oscillatory increase (lower trace). The peak fluorescence for each experiment is 5× as great as the respective control value.

(C) Cells stably transfected with chicken VR-OAC produce graded responses to a range of hypotonic solutions. The data points represent an exchange from isotonic solution (295 mmol·kg<sup>-1</sup>) to solutions with osmotic strengths (in mmol·kg<sup>-1</sup>) of 223 (diamonds), 247 (triangles), 259 (squares), 273 (filled circles), 288 (stars), and 295 (open circles). The stimulus period is indicated below the traces. The peak fluorescence is 4.6× as great as the control value.

(D) The temperature sensitivity of cell lines stably transfected with rat or chicken VR-OAC is demonstrated by the fluorescence from roughly 2000 cells stimulated with hypotonic solution of 260 mmol·kg<sup>-1</sup>. Data are presented as means and standard deviations from 3–4 measurements. For rat VR-OAC, the sensitivity peaks at 37°C, the mammalian core body temperature; for chicken VR-OAC, maximal responsiveness occurs at 40°C, the avian core body temperature. RT, room temperature.

(E) In a control experiment, internal Ca<sup>2+</sup> stores are depleted with 10 μM thapsigargin and potentiation channels are blocked with 20 μM SKF 96365. Under these conditions, the modest background level of fluo-4 fluorescence does not increase upon exposure to hypotonic medium.

(F) When transfected cells in isotonic medium free of Ca<sup>2+</sup> are exposed to Ca<sup>2+</sup>-free hypotonic medium, no change occurs in the intracellular fluo-4 fluorescence. When 2 mM Ca<sup>2+</sup> is added to the medium, however, the intracellular Ca<sup>2+</sup> concentration promptly rises.

stretch-activated channels (Yang and Sachs, 1989). Within the first few minutes of extracellular application, the effect of 500 μM Gd<sup>3+</sup> on VR-OAC-transfected cells resembled that of Ca<sup>2+</sup>. More protracted exposure to Gd<sup>3+</sup> irreversibly abolished the whole-cell current (not

shown). Similar observations were made by inside-out patch recordings. The slow development of the Gd<sup>3+</sup>-dependent block suggests that the ion suppresses conduction in VR-OACs through an indirect mechanism, rather than by tightly binding in the pore. Consistent

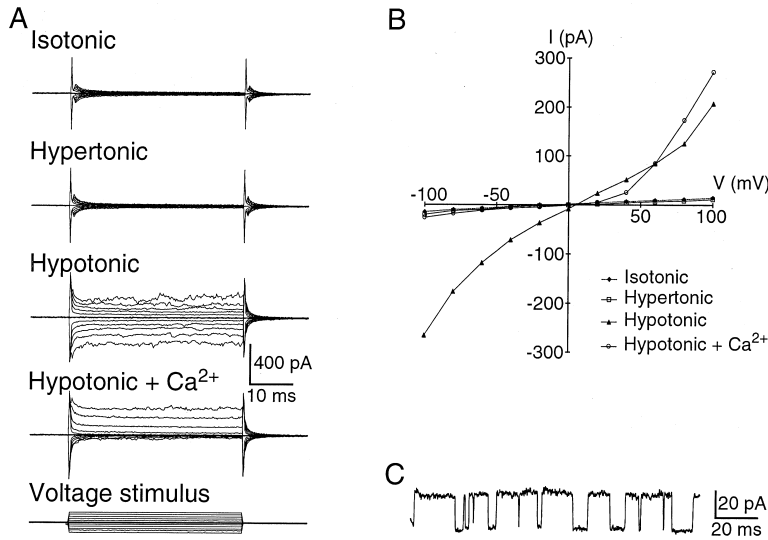


Figure 7. Electrophysiological Characterization of VR-OAC-Expressing CHO Cells

(A) Whole-cell current responses to voltage-step stimuli illustrate the osmotic sensitivity and  $\text{Ca}^{2+}$ -dependent rectification of VR-OAC. The membrane potential was held at 0 mV and stepped in 20 mV increments to  $\pm 100$  mV (bottom family of traces). Cells exposed to isotonic or hypertonic solutions responded similarly to untransfected control cells. Hypotonic solutions, however, elicited robust whole-cell currents with marked outward rectification in the presence of 1 mM free  $\text{Ca}^{2+}$ . The rectification developed rapidly and disappeared immediately upon withdrawal of  $\text{Ca}^{2+}$ .

(B) The voltage-current relation under hypotonic conditions displays dual rectification. Inclusion of  $\text{Ca}^{2+}$  in the hypotonic medium significantly reduces the inward current.

(C) A current record from an inside-out patch at +80 mV shows unitary events corresponding to a conductance of 310 pS. The upper level represents the channel's open state. Although the results shown were taken from chicken VR-OAC recordings, the electrophysiological responses of the rat ortholog corroborated the principal conclusions.

results were obtained by fluo-4 imaging during  $\text{Gd}^{3+}$  application.

In patch recordings from VR-OAC-expressing cells, we observed large single-channel currents (Figure 7C) never encountered in control cells. On the basis of clearly defined unitary currents, the single-channel conductance of VR-OAC is 310 pS. In both inside-out and outside-out excised patches containing multiple channels, gating exhibited strong voltage dependence. Because the current during the largest voltage steps was often smaller than the response to smaller stimuli, the channels may display inactivation.

We performed a control experiment to confirm that the current through VR-OACs was unchanged under conditions in which the internal  $\text{Ca}^{2+}$  stores had been depleted. After incubation in 10  $\mu\text{M}$  thapsigargin and 20  $\mu\text{M}$  SKF 96365, cells displayed characteristic VR-OAC currents when stimulated with hypotonic solution. Like VR1 (Caterina et al., 1997), VR-OAC is therefore not a store-operated channel.

#### Deletion of the Ankyrin-Repeat Domain

The amino-terminal domain of VR-OAC includes three ankyrin repeats that might physically link the receptor to the cytoskeleton (Figures 1 and 2A). To evaluate the potential importance of this domain, we constructed two VR-OAC variants: eGFP-OAC, which bears the complete coding sequence of rat VR-OAC fused at its amino terminus to the carboxyl terminus of enhanced green fluorescent protein (eGFP), and eGFP- $\Delta$ OAC, a similar construct lacking the first 402 amino acids of VR-OAC, including all three ankyrin repeats. Confocal microscopy of transiently and stably transfected cells indicated that both the intact and deleted fusion proteins were localized to the plasma membrane. The fusion proteins sometimes produced membrane-associated fluorescent clusters that did not colocalize with focal adhesion

points visualized by paxillin immunolabeling (not shown).

Both eGFP-OAC and eGFP- $\Delta$ OAC responded to hypotonic stimuli. Electrophysiological evaluation of osmotically stimulated cells expressing the two fusion proteins and native VR-OAC disclosed no significant differences in their steady-state responses to hypotonic stimulation (not shown).  $\text{Ca}^{2+}$ -imaging experiments revealed, however, that cells expressing the fusion protein without ankyrin repeats responded less robustly than cells expressing the intact variant during the first 60 s after application of a hypotonic stimulus. The ratio of fluorescence 60 s after stimulus application to that before stimulation differed significantly ( $p < 0.01$ , Student's *t* test) between cells transfected with GFP-OAC ( $4.4 \pm 2.1$ , mean  $\pm$  standard deviation,  $n = 7$ ) and eGFP- $\Delta$ OAC ( $0.8 \pm 0.4$ ,  $n = 8$ ).

#### Discussion

Although osmoreception and mechanoreception occur at numerous locations in the vertebrate nervous system, the identity of the receptor molecules is unknown. In this report, we present evidence that VR-OAC acts *in vitro* as a poorly selective vertebrate cation channel that is gated by osmotic stress. Among the cell types that express VR-OAC are neurosensory cells that have previously been demonstrated to respond to systemic osmotic pressure. Because osmosensitivity is thought to stem from the detection of membrane tension by mechanosensitive channels, VR-OACs might be expected to respond to other mechanical stimuli as well. Consistent with this hypothesis, VR-OACs occur in mechanosensory cells of the inner ear and the somatosensory system.

VR-OAC belongs to the OSM-9 family of the TRP superfamily of ion channels, whose members respond to

ligands (VR1), heat (VR1 and VRL-1), and osmotic stimuli (OSM-9 and VR-OAC). In *C. elegans*, the single protein OSM-9 mediates responsiveness to ligands, osmotic pressure, and touch; heat has not been tested (Colbert et al., 1997). The gene ancestral to *Osm-9* was presumably replicated several times during vertebrate evolution, so that the sensory functions mediated by OSM-9 have been distributed among at least three different proteins, VR1, VRL-1, and VR-OAC. VR-OAC is also distantly related to the mechanosensitive channel NOMPC in *Drosophila*, but has no homology with the mechanosensitive channel MID1 in yeast or with the putative channel components MEC-4 and MEC-10 in *Caenorhabditis*.

#### Gating of VR-OAC

Our experiments establish that osmotic stimuli, presumably acting through membrane stretch, efficiently gate VR-OAC. Although the response of VR-OAC to osmotic strengths slightly below the physiological setpoint supports the relevance of subtle changes in membrane tension as an effective stimulus, the gating mechanism of VR-OAC is unknown. The relatively normal sensitivity of the mutant receptor lacking the ankyrin repeats implies that an ankyrin-mediated connection to the cytoskeleton is not essential for gating by osmotic stress, but a connection might be required for rapid responsiveness. VR-OAC might be part of a multimeric complex in which a binding partner provides additional anchoring to the cytoskeleton so that VR-OAC lacking its ankyrin repeats nevertheless responds.

VR-OAC is the first osmotically activated channel to be characterized in vertebrates. A fuller understanding of its function in vivo awaits the results of analysis of gene-targeted mice. However, the functional properties obtained upon heterologous expression of VR-OAC and the localization of its mRNA suggest several possibilities that are discussed below.

#### Potential Relevance of VR-OAC for Systemic Osmoregulation

Systemic osmotic pressure is one of the most aggressively defended setpoint values in vertebrate animals. Osmoregulation by the central nervous system thus constitutes a homeostatic circuit of vital significance. In the nuclei of the central nervous system that are known to function in osmoregulation, VR-OAC is expressed in neurons of two circumventricular organs, the vascular organ of the *lamina terminalis* (VOLT) and the subfornical organ (SFO). The circumventricular organs represent the only part of the brain lacking a blood-brain barrier (McKinley and Oldfield, 1990). VOLT and SFO neurons, which respond to changes in osmotic pressure, project to the antidiuretic hormone-secreting magnocellular neurosecretory cells in the supraoptic and paraventricular nuclei of the hypothalamus (Sibbald et al., 1988; McKinley et al., 1992; Denton et al., 1996; Bourque and Oliet, 1997). VOLT and SFO are thus regarded as osmoreceptive sensory organs within the central nervous system. Lesioning experiments have established a role for the VOLT and SFO in osmotically induced drinking behavior (Thrasher et al., 1982; McKinley et al., 1999).

In support of the hypothesis that VR-OAC serves as an osmoreceptor responsive to systemic hypotonicity,

expression in the VOLT corresponds with peroxidase labeling that signals the absence of a blood-brain barrier (Bisley et al., 1996). Moreover, the sensitivity of VR-OAC is maximal at the core body temperature and lies within the physiological range of osmoregulation.

The third part of the *lamina terminalis* that bears VR-OAC-expressing neurons, the median preoptic area (MnPO), differs from the VOLT and SFO by possessing an intact blood-brain barrier. The MnPO has nevertheless been implicated in osmotically induced drinking behavior and in adaptive responses leading to the secretion of antidiuretic hormone (Travis and Johnson, 1993). It is plausible that MnPO neurons sense circulatory osmolality in the adjacent VOLT and SFO by means of osmoreceptor-bearing axonal projections into those areas.

The occurrence of VR-OAC in the choroid plexus of the lateral ventricles suggests a role in sensing the hydrostatic or osmotic pressure of cerebrospinal fluid (McKinley and Oldfield, 1990). The expression of VR-OAC in the kidney by tubular cells, and to a lesser degree by glomerular cells, also fits with a postulated osmosensory function of the channel.

#### Potential Relevance of VR-OAC for Inner-Ear Function

In the cochlea, expression of VR-OAC mRNA was detected in marginal cells of the *stria vascularis*, nonsensory cells that maintain the ionic composition of endolymph and the endocochlear potential. VR-OAC in these cells could participate in regulation of the osmotic or hydrostatic pressure in the endolymph. VR-OAC mRNA was also detected in cochlear outer and inner hair cells and in vestibular hair cells. The channel might therefore act as an osmotic sensor in the fluid homeostasis of these cells.

Might VR-OAC form the hair cell's mechano-electrical transduction channel? The channel's physiological properties, including voltage sensitivity and a single-channel conductance of 310 pS, make this role improbable for VR-OAC alone. The VR-OAC protein could, however, be part of a heteromultimeric transduction channel. It might alternatively mediate a second form of mechanosensitivity in hair cells, the slow mechanical response that persists after tip-link disruption (Meyer et al., 1998). It is interesting in this context that *nompC* null mutants display a small mechanoreceptor potential (Walker et al., 2000) that might be caused by the *Drosophila* ortholog of VR-OAC.

#### Potential Relevance of VR-OAC for Somatosensory Function

VR-OAC mRNA is abundantly expressed by a subpopulation of large neurons in the trigeminal ganglion. The labeled cells include neither the small sensory neurons that give rise to unmyelinated C fibers nor the very large neurons whose A $\alpha$  (class I) fibers innervate muscle spindles. VR-OAC mRNA occurs in neurons whose myelinated, rapidly conducting A $\gamma$  (class II) and A $\delta$  (class III) fibers mediate epicritic mechanosensation. It is noteworthy that the maximal sensitivity of VR-OAC at normal body temperatures (Figure 6D) corresponds to the peak thermal sensitivity for tactile and vibratory stimuli in

mammals (Weitz, 1941; Fucci et al., 1976; Dehnhardt et al., 1998).

We also observed VR-OAC mRNA in the Merkel cells associated with vibrissae. Because of their synaptic contacts with sensory nerve endings, Merkel cells have been suggested to be mechanoreceptors (Andres and von Düring, 1973).

In summary, we identified an osmotically activated channel in the rat, mouse, human, and chicken. The anatomical distribution of the novel channel suggests that it plays a role in sensing systemic osmotic pressure and the osmotic or hydrostatic pressure in several physiological compartments of the body.

## Experimental Procedures

### Cloning of VR-OAC

A cDNA encoding VR-OAC was identified in a rat kidney library (Tate et al., 1992) through screening with a 283 base-pair fragment derived from W53556, an expressed sequence tag with homology to VR1. Two million clones of a mouse hypothalamus cDNA library were screened with a mixture of nucleotide probes corresponding to the transmembrane regions of VR1, VRL-1, and OSM-9. Two 2.6 kb clones harbored an incomplete mouse VR-OAC cDNA. The missing 5' end was retrieved through 5'-RACE (Clontech Laboratories, Palo Alto, CA).

221,184 randomly selected clones from a chicken auditory epithelium cDNA library (Heller et al., 1998) were arrayed on nylon filters (Genome Systems/Incyte Genomics Inc., St. Louis, MO). The resulting macroarrays were screened with <sup>32</sup>P-labeled probes in a fashion similar to that used for the hypothalamic cDNA library. One clone contained the full-length coding sequence of chicken VR-OAC. Six additional chicken VR-OAC cDNAs were isolated by conventional plaque hybridization from the original chicken library.

Amino acid sequences were analyzed using the PSI-BLAST algorithm (<http://www.ncbi.nlm.nih.gov>), PSORT (<http://psort.nibb.ac.jp>), the PHDsec program (Rost and Sander, 1993), and PHYLIP (Retief, 2000).

### Expression Analysis

Northern blot analysis was performed with a <sup>32</sup>P-dCTP-labeled cDNA probe corresponding to nucleotides 384–667 of the rat *Vroac* cDNA. In situ hybridization was performed on frozen sections according to established protocols (Heller et al., 1998; <http://dir.niehs.nih.gov/dirlep/ish.html>). Two mouse VR-OAC mRNA-specific antisense riboprobes were used, one corresponding to nucleotides 384–667, encoding the amino terminus, and another corresponding to nucleotides 1401–1746, encoding the first two transmembrane domains. The respective sense probes served as controls.

Immunocytochemistry was performed according to established protocols (Liedtke et al., 1996) and the manufacturers' suggestions (<http://www.zymed.com>; <http://home.att.net/~sternbmonoc/SMI35.htm>).

### Chromosomal Mapping

Radiation hybrid panel mapping was conducted with the T31 mouse-hamster genomic DNA hybrid cell line panel (Research Genetics, Huntsville, AL). A mouse-hamster polymorphism based on *Vroac* cDNA nucleotides 384–501 was used for the PCR.

To map *Vr1*, we amplified from mouse genomic DNA an intronic sequence between nucleotides 2082 and 2346. Using as templates *Mus spretus* and *M. musculus* BL6 genomic DNA, we employed an XbaI polymorphism to type the JAX BSS backcross panel, (C57BL/6Jei × SPRET/Ei)F1 × SPRET/Ei (Rowe et al., 1994).

### Cell Lines and Ca<sup>2+</sup>-Imaging Experiments

The complete cDNAs of rat VR-OAC, chicken VR-OAC, and rat VR1 were subcloned into the eukaryotic expression vector pcDNA3.1 (Invitrogen, Carlsbad, CA). CHO-K1 cells (ATCC, Manassas, VA) were transfected with these vectors and selected with G418 (Life Technology, Gaithersburg, MD). Stable clones that expressed the

mRNAs were identified by Northern blot analysis and, for VR1, by response to ligand.

For Ca<sup>2+</sup> imaging, cells were plated on glass-bottom dishes 36–48 hr prior to the experiment and loaded with fluo-4 by incubation for 30 min at room temperature in 1.5 mM of the acetoxymethyl ester (Molecular Probes, Eugene, OR) in isoosmotic saline solution containing 130 mM Na<sup>+</sup>, 2.5 mM K<sup>+</sup>, 2 mM Ca<sup>2+</sup>, 1 mM Mg<sup>2+</sup>, 138.5 mM Cl<sup>-</sup>, 20 mM D-glucose, and 10 mM HEPES at pH 7.3 (Babcock et al., 1997).

Confocal analysis was performed with an MRC-1024ES system (Bio-Rad, Hercules, CA) mounted on an inverted microscope (Zeiss Axiovert 135TV, Carl Zeiss, Jena, Germany). Analysis of single-frame or single-cell integrated signal density was performed on Macintosh computers running NIH Image software (version 1.61; O'Neill et al., 1989).

Solutions with different osmotic strengths were created by adding water or mannitol to the saline solution. Unless otherwise noted, the Ca<sup>2+</sup> concentration of all solutions was held constant at 2 mM. Osmolalities were verified with a vapor-pressure osmometer (Vapro 5520, Wescor Inc., Logan, UT). The test solutions included a graded series of hypotonic solutions (with 220 mmol·kg<sup>-1</sup> the lowest osmolality), a hypertonic solution (330 mmol·kg<sup>-1</sup>), isotonic solutions at 295 mmol·kg<sup>-1</sup> with graded concentrations of Na<sup>+</sup> (with 50 mM the lowest concentration), and hypotonic solutions containing 100 μM, 250 μM, and 500 μM GdCl<sub>3</sub>. Ligands used for stimulation were resiniferatoxin (Sigma Chemicals, St. Louis, MO) at 0.2 μM and 5 μM and anandamide (Cayman Chemical, Ann Arbor, MI) at 5 μM and 25 μM. To test whether VR-OAC is directly gated by increases in temperature, we exposed dishes containing fluo-4-loaded cells to temperatures ranging from room temperature to 30°C, 37°C, 40°C, 45°C, 50°C, and 55°C. Images were acquired during the thermal stimulus series at intervals of 60 s for up to 10 min after the start of heating. A series of calibration experiments confirmed that this interval ensured proper thermal equilibration. A similar procedure was used to test the response to hypotonicity at various temperatures.

### Electrophysiological Recordings

Electrophysiological characterization of VR-OAC was performed at room temperature on CHO cell lines stably or transiently transfected with one of four expression vectors, pcDNA3.1 (Invitrogen) with inserts bearing chicken or rat VR-OAC, eGFP-OAC, or eGFP-ΔOAC. These cells were selected because untransfected HEK 293 cells responded to hypotonic stress and *Xenopus laevis* oocytes are sensitive to membrane stretch (Yang and Sachs, 1989).

Cells plated on glass-bottom Petri dishes were observed through a 40× water-immersion objective lens on an inverted microscope equipped with Nomarski optics. Tight-seal pipettes were bent to permit an orthogonal approach to a cell's surface and heat-polished to give resistances of 3–5 MΩ. Internal solutions typically contained 117 mM NaCl, 5 mM HEPES, 1 mM EDTA, and mannitol to achieve isotonicity. Whole-cell and patch currents were recorded with a voltage-clamp amplifier (EPC-7, List-Electronic, Darmstadt-Eberstadt, Germany). Cells were generally held at -60 mV. Pipette and cell capacitances were largely compensated; series-resistance compensation ranged from 10% to 60%. Responses were low-pass filtered at 2 kHz with an eight-pole Bessel filter and sampled at 5 kHz.

During whole-cell recording, cells were maintained in isotonic or slightly hypertonic solutions. Stimulation was accomplished by perfusion of hypotonic solutions and measurements were performed within 5 min of stimulation. The standard hypotonic solution contained 117 mM NaCl, 5 mM HEPES, and 1 mM EDTA and had an osmotic strength of 225 mmol·kg<sup>-1</sup>. Isotonic and hypertonic solutions were prepared by supplementing this hypotonic solution with mannitol to, respectively, 295 mmol·kg<sup>-1</sup> and 340 mmol·kg<sup>-1</sup>. All solutions used in perfusion of cells had a pH of 7.3 and contained 1 mM phenol red for visibility. EDTA did not appear to have deleterious effects on the cells, for whole-cell currents could be recorded stably for over 20 min.

In studies of the effects of Ca<sup>2+</sup> and Gd<sup>3+</sup> on whole-cell currents, hypotonic test solutions included, respectively, 2 mM CaCl<sub>2</sub> or 500 μM GdCl<sub>3</sub>. Because carboxylic-acid Ca<sup>2+</sup> chelators compromise the

capacity of  $GdCl_3$  to block mechanosensitive channels (Caldwell et al., 1998), EDTA was excluded from the latter medium and the pipette solution. Inside-out and outside-out patch recordings were performed with isotonic NaCl solution lacking EDTA in the pipette and an identical solution supplemented with 1 mM  $CaCl_2$  in the bath.

#### Acknowledgments

We thank Dr. S. S. Tate for the rat kidney cDNA library, Dr. C. Bargmann for the OSM-9 cDNA, Drs. L. Rowe and M. Barter for their assistance with murine gene mapping, and Drs. Z. -P. Sun, N. Heintz, and D. Gadsby for valuable discussions. This work was supported by National Institutes of Health grants GM54762, DC00317, and DK41096. Y. C. was supported in part by a graduate fellowship from the National Science Foundation. A. Š. is a Fellow of the Alfred P. Sloan Foundation, and J. M. F. and A. J. H. are Investigators of Howard Hughes Medical Institute.

Received May 10, 2000; revised October 2, 2000.

#### References

- Andres, K.H., and von Düring, M. (1973). Morphology of cutaneous receptors. In *Handbook of Sensory Physiology, Volume II, Somatosensory System*, A. Iggo, ed. (Berlin, Germany: Springer), pp. 3–28.
- Babcock, D.F., Herrington, J., Goodwin, P.C., Park, Y.B., and Hille, B. (1997). Mitochondrial participation in the intracellular  $Ca^{2+}$  network. *J. Cell Biol.* 136, 833–844.
- Bisley, J.W., Rees, S.M., McKinley, M.J., Hards, D.K., and Oldfield, B.J. (1996). Identification of osmoreponsive neurons in the forebrain of the rat: a Fos study at the ultrastructural level. *Brain Res.* 720, 25–34.
- Bourque, C.W., and Oliet, S.H. (1997). Osmoreceptors in the central nervous system. *Annu. Rev. Physiol.* 59, 601–619.
- Caldwell, R.A., Clemo, H.F., and Baumgarten, C.M. (1998). Using gadolinium to identify stretch-activated channels: technical considerations. *Am. J. Physiol.* 275, C619–C621.
- Caterina, M.J., and Julius, D. (1999). Sense and specificity: a molecular identity for nociceptors. *Curr. Opin. Neurobiol.* 9, 525–530.
- Caterina, M.J., Schumacher, M.A., Tominaga, M., Rosen, T.A., Levine, J.D., and Julius, D. (1997). The capsaicin receptor: a heat-activated ion channel in the pain pathway. *Nature* 389, 816–824.
- Caterina, M.J., Rosen, T.A., Tominaga, M., Brake, A.J., and Julius, D. (1999). A capsaicin-receptor homologue with a high threshold for noxious heat. *Nature* 398, 436–441.
- Colbert, H.A., Smith, T.L., and Bargmann, C.I. (1997). OSM-9, a novel protein with structural similarity to channels, is required for olfaction, mechanosensation, and olfactory adaptation in *Caenorhabditis elegans*. *J. Neurosci.* 17, 8259–8269.
- Dehnhardt, G., Mauck, B., and Hyvarinen, H. (1998). Ambient temperature does not affect the tactile sensitivity of mystacial vibrissae in harbour seals. *J. Exp. Biol.* 201, 3023–3029.
- Denton, D.A., McKinley, M.J., and Weisinger, R.S. (1996). Hypothalamic integration of body fluid regulation. *Proc. Natl. Acad. Sci. USA* 93, 7397–7404.
- Eppley, Z. (1996). Development of thermoregulation in birds: physiology, interspecific variation and adaptation to climate. In *Animals and Temperature, Phenotypic and Evolutionary Adaptation*, I. A. Johnston and A. F. Bennett, eds. (Cambridge, United Kingdom: Cambridge University Press), pp. 313–345.
- French, A.S. (1992). Mechanotransduction. *Annu. Rev. Physiol.* 54, 135–152.
- Fucci, D., Cray, M., and Wilson, H. (1976). Vibrotactile and temperature sensory interaction in the human tongue. *Percept. Mot. Skills* 43, 263–266.
- Gu, G., Caldwell, G.A., and Chalfie, M. (1996). Genetic interactions affecting touch sensitivity in *Caenorhabditis elegans*. *Proc. Natl. Acad. Sci. USA* 93, 6577–6582.
- Harteneck, C., Plant, T.D., and Schultz, G. (2000). From worm to man: three subfamilies of TRP channels. *Trends Neurosci.* 23, 159–166.
- Heller, S., Sheane, C.A., Javed, Z., and Hudspeth, A.J. (1998). Molecular markers for cell types of the inner ear and candidate genes for hearing disorders. *Proc. Natl. Acad. Sci. USA* 95, 11400–11405.
- Hudspeth, A.J., and Gillespie, P.G. (1994). Pulling springs to tune transduction: adaptation by hair cells. *Neuron* 12, 1–9.
- Kanzaki, M., Nagasawa, M., Kojima, I., Sato, C., Naruse, K., Sokabe, M., and Iida, H. (1999). Molecular identification of a eukaryotic, stretch-activated nonselective cation channel. *Science* 285, 882–886.
- Kernan, M., and Zuker, C. (1995). Genetic approaches to mechanosensory transduction. *Curr. Opin. Neurobiol.* 5, 443–448.
- Lai, C.C., Hong, K., Kinnell, M., Chalfie, M., and Driscoll, M. (1996). Sequence and transmembrane topology of MEC-4, an ion channel subunit required for mechanotransduction in *Caenorhabditis elegans*. *J. Cell Biol.* 133, 1071–1081.
- Liedtke, W., Edelman, W., Bieri, P.L., Chiu, F.-C., Cowan, N.J., Kuchlerlpati, R., and Raine, C.S. (1996). GFAP is necessary for the integrity of CNS white matter architecture and long-term maintenance of myelination. *Neuron* 17, 607–615.
- McKinley, M.J., and Oldfield, B.J. (1990). Circumventricular organs. In *The Human Nervous System*, G. Paxinos, ed. (San Diego, California: Academic Press), pp. 415–438.
- McKinley, M.J., Bicknell, R.J., Hards, D., McAllen, R.M., Vivas, L., Weisinger, R.S., and Oldfield, B.J. (1992). Efferent neural pathways of the lamina terminalis subserving osmoregulation. *Prog. Brain Res.* 97, 395–402.
- McKinley, M.J., Mathai, M.L., Pennington, G., Rundgren, M., and Vivas, L. (1999). Effect of individual or combined ablation of the nuclear groups of the lamina terminalis on water drinking in sheep. *Am. J. Physiol.* 276, R673–R683.
- Merritt, J.E., Armstrong, W.P., Benham, C.D., Hallam, T.J., Jacob, R., Jaxa-Chamiec, A., Leigh, B.K., McCarthy, S.A., Moores, K.E., and Rink, T.J. (1990). SK&F 96365, a novel inhibitor of receptor-mediated calcium entry. *Biochem. J.* 271, 515–522.
- Meyer, J., Furness, D.N., Zenner, H.P., Hackney, C.M., and Gummer, A.W. (1998). Evidence for opening of hair-cell transducer channels after tip-link loss. *J. Neurosci.* 18, 6748–6756.
- O'Neill, R.R., Mitchell, L.G., Merril, C.R., and Rasband, W.S. (1989). Use of image analysis to quantitate changes in form of mitochondrial DNA after x-irradiation. *Appl. Theor. Electrophor.* 1, 163–167.
- Penner, R., Neher, E., Takeshima, H., Nishimura, S., and Numa, S. (1989). Functional expression of the calcium release channel from skeletal muscle ryanodine receptor cDNA. *FEBS Lett.* 259, 217–221.
- Retief, J.D. (2000). Phylogenetic analysis using PHYLIP. *Methods Mol. Biol.* 132, 243–258.
- Rost, B., and Sander, C. (1993). Prediction of protein secondary structure at better than 70% accuracy. *J. Mol. Biol.* 232, 584–599.
- Rowe, L.B., Nadeau, J.H., Turner, R., Frankel, W.N., Letts, V.A., Eppig, J.T., Ko, M.S., Thurston, S.J., and Birkenmeier, E.H. (1994). Maps from two interspecific backcross DNA panels available as a community genetic mapping resource. *Mamm. Genome* 5, 253–274.
- Sackin, H. (1995). Mechanosensitive channels. *Annu. Rev. Physiol.* 57, 333–353.
- Sibbald, J.R., Hubbard, J.I., and Sirett, N.E. (1988). Responses from osmosensitive neurons of the rat subfornical organ in vitro. *Brain Res.* 461, 205–214.
- Sukharev, S.I., Blount, P., Martinac, B., Blattner, F.R., and Kung, C. (1994). A large-conductance mechanosensitive channel in *E. coli* encoded by *mscL* alone. *Nature* 368, 265–268.
- Tate, S.S., Yan, N., and Udenfriend, S. (1992). Expression cloning of a Na(+)-independent neutral amino acid transporter from rat kidney. *Proc. Natl. Acad. Sci. USA* 89, 1–5.
- Thrasher, T.N., Keil, L.C., and Ramsay, D.J. (1982). Lesions of the organum vasculosum of the lamina terminalis (OVLT) attenuate osmotically-induced drinking and vasopressin secretion in the dog. *Endocrinology* 110, 1837–1839.
- Touchman, J.W., Anikster, Y., Dietrich, N.L., Maduro, V.V., McDowell, G., Shotelersuk, V., Bouffard, G.G., Beckstrom-Sternberg, S.M., Gahl, W.A., and Green, E.D. (2000). The genomic region encom-

passing the nephropathic cystinosis gene (CTNS): complete sequencing of a 200-kb segment and discovery of a novel gene within the common cystinosis-causing deletion. *Genome Res.* *10*, 165–173.

Travis, K.A., and Johnson, A.K. (1993). In vitro sensitivity of median preoptic neurons to angiotensin II, osmotic pressure, and temperature. *Am. J. Physiol.* *264*, R1200–R1205.

Walker, R.G., Willingham, A.T., and Zuker, C.S. (2000). A *Drosophila* mechanosensory transduction channel. *Science* *287*, 2229–2234.

Weitz, J. (1941). Effect of temperature on sensitivity of the finger. *J. Exp. Psychol.* *28*, 21–36.

Yang, X.C., and Sachs, F. (1989). Block of stretch-activated ion channels in *Xenopus* oocytes by gadolinium and calcium ions. *Science* *243*, 1068–1071.

Zygmunt, P.M., Petersson, J., Andersson, D.A., Chuang, H., Sorgard, M., Di Marzo, V., Julius, D., and Hogestatt, E.D. (1999). Vanilloid receptors on sensory nerves mediate the vasodilator action of anandamide. *Nature* *400*, 452–457.

#### **GenBank Accession Numbers**

The rat, mouse, human, and chicken cDNA sequences for VR-OAC described in this paper are entered in GenBank under accession numbers AF263521, AF263522, AF263523, and AF261883, respectively.